Intracellular Trafficking and Dynamics of Double Homeodomain Proteins†

Cecilia Östlund,‡ Ruth M. Garcia-Carrasquillo,‡ Alexandra Belayew,§ and Howard J. Worman*,‡

Department of Medicine and Department of Anatomy and Cell Biology, College of Physicians and Surgeons, Columbia University, Room 10-509, 630 West 168th Street, New York, New York 10032, and Laboratory of Molecular Biology, University of Mons-Hainaut, Pentagone 3A, Avenue du Champ de Mars 6, B-7000, Mons, Belgium

Received September 17, 2004; Revised Manuscript Received November 16, 2004

ABSTRACT: Double homeodomain (DUX) proteins are encoded by a family of 3.3-kilobase repeated elements dispersed in the human genome. One of these elements named D4Z4 is found in a tandem repeat array on chromosome 4 that is partially deleted in facioscapulohumeral muscular dystrophy. We have evaluated the trafficking and mobility of two DUX proteins, DUX1 and DUX4. We transfected C2C12 myoblasts with cDNA encoding these proteins fused to the green fluorescent protein and studied their intracellular localization and diffusional mobilities using fluorescence recovery after photobleaching and fluorescence loss in photobleaching. We also studied truncated forms of the proteins, containing one or both homeodomains or a region outside the homeodomains. We show that both full-length proteins are actively transported into the nucleus, and that the homeodomains contain the signals required for this localization. DUX1 is more mobile than DUX4 within the nucleus ($t_{1/2}$ = 4.8 s for DUX1 and 13.4 s for DUX4), suggesting differences in the way the two proteins interact with nuclear components.

Homeodomain proteins are transcription factors containing a conserved DNA-binding helix−turn−helix domain of 60 amino acids, encoded by the 180 base pair homeobox sequence (*1*). This sequence was first identified in *Drosophila* genes essential for normal development (*2*). Later studies have identified homeobox genes in fungi, plants, and other animals and have shown that their functions are not limited to roles in development and differentiation, but that they also play important roles in diseases such as diabetes and cancer (*3*, *4*). The homeodomain has three α-helical segments, with the third being the recognition domain, which interacts with the major groove of DNA and is important for the sequence specificity of DNA recognition (*1*).

The *DUX* genes encode a family of proteins with double homeodomains (*5*−*7*). Their homeodomains are most closely related to those of the *Siamois* family of paired-like type homeodomain proteins (*5*, *8*, *9*). *DUX* genes are present in 3.3-kilobase elements, a tandem repeat family scattered in the human genome found on the short arms of all acrocentric chromosomes as well as on several other chromosomes (*5*, *7*, *10*, *11*). Of particular interest are the repeats on chromosome 4, named D4Z4, as deletions of the majority of these are associated with facioscapulohumeral muscular dystrophy (FSHD)[1], the third most common form of inherited muscular dystrophy (*12*−*14*). It has been hypothesized that the large D4Z4 copy number found in nonaffected individuals is associated with an inhibitory chromatin structure preventing gene expression. This inhibition would be relieved in the shorter repeat arrays linked to the disease (*10*). The *DUX4* gene was identified in the two D4Z4 elements left by an FSHD inducing deletion in a patient, and it was hypothesized that DUX4 was expressed in patient myoblasts (*6*).

DUX1 is a protein of 170 amino acids expressed in human rhabdomyosarcoma TE671 cells as well as in several other normal and cancer cells (*5*, *7*, The Cancer Genome Anatomy Project http://cgap.nci.nih.gov). It contains two homeodomains flanked by short amino-terminal and carboxyl-terminal regions. Different polymorphic forms of the DUX1 protein are encoded by the *DUX3* and *DUX5* genes, present on the acrocentric chromosomes (*7*). These chromosomes also contain the *DUX2* gene, which encodes DUX2 (*7*), a shorter protein with only one homeodomain 71% identical to the amino-terminal region of DUX1 and 87% identical to the amino-terminal region of DUX4. The amino-terminal region of DUX4, containing the homeodomains and flanking regions, is highly homologous to DUX1 (84%), but DUX4, which extends over 424 residues, has a longer carboxyl-terminal region (*6*). DUX4 is expressed in HCT-116 colon cancer cells with two major methyltransferases genetically disrupted, while the expression of the gene is suppressed by hypermethylation in the parent cell line (*15*). DUX4 expression has not been reported in normal cells and tissues. Recently, a protein with the expected charge (p*I* 8.6) and apparent molecular mass (52 kDa) of DUX4 was detected in primary myoblast extracts from subjects with FSHD, but not in controls, by two-dimensional gel electrophoresis and western blot with an antiserum raised against the double homeodomain (*16*).

† C.Ö. was supported by FSH Society Grant FSHS-MB-008, and A.B. and H.J.W. were supported by NIH Grant NS046242.

* Corresponding author: e-mail, hjw14@columbia.edu; phone, 212-305-8156; fax, 212-305-6443.

‡ Columbia University.

§ University of Mons-Hainaut.

[1] Abbreviations: DUX, double homeodomain protein; FITC, fluorescein isothiocyanate; FLIP, fluorescence loss in photobleaching; FRAP, fluorescence recovery after photobleaching; FSHD, facioscapulohumeral muscular dystrophy; GFP, green fluorescent protein; HP1, heterochromatin protein 1; NLS, nuclear localization signal; NPC, nuclear pore complex; PBS, phosphate-buffered saline.

10.1021/bi047992w CCC: $30.25
Published on Web 01/25/2005

Homeodomain proteins are localized to the cell nucleus. In most cases, this location is dependent on a nuclear localization signal (NLS) residing within the homeodomain (*17*−*19*). Defects in such signals contribute to human diseases such as Bloom syndrome and Werner syndrome (*18*, *20*, *21*). Recent work has shown that the paired-type homeodomain proteins Pax3, Pax6, and Crx are imported into the nucleus by the transport factor karyopherin 13, and that regions at each end of the homeodomain containing several basic amino acids are important for this process (*22*). However, there are no published studies on the intracellular trafficking of double homeodomain proteins and the intracellular localizations of DUX proteins are not known. In this study, we investigate trafficking of the double homeodomain proteins DUX1 and DUX4 and their diffusional mobilities in different compartments of the cell.

EXPERIMENTAL PROCEDURES

Plasmid Construction. All cloning procedures were performed according to standard methods (*23*). cDNAs were generated by the polymerase chain reaction (*24*) using the Geneamp PCR System 9700 (Applied Biosystems, Foster City, CA) with restriction sites engineered at the 5′ ends of the primers. DUX1 cDNA and a genomic fragment from a D4Z4 repeat encoding DUX4 in vector pCI-neo were used as templates (*5*, *6*). Constructs expressing DUX proteins fused to green fluorescent protein (GFP) were made in plasmid pEGFP-N2 (Clontech, Palo Alto, CA), which contains a multiple cloning site downstream from the cytomegalovirus promoter and upstream of the sequence encoding enhanced GFP. cDNAs were generated with an *Eco*RI restriction site at the 5′ end and a *Kpn*I restriction site at the 3′ end and ligated into the *Eco*RI and *Kpn*I restriction sites of pEGFP-N2. Constructs expressing DUX proteins fused to a FLAG-tag were made in pSVF, a vector constructed by insertion of the FLAG-epitope coding sequence between the *Eco*RI and *Kpn*I restriction sites of pSVK3 (Amersham Pharmacia Biotech, Inc., Piscataway, NJ). cDNAs were generated with a *Kpn*I site at the 5′ end and a stop-codon and a *Xho*I site at the 3′ end. They were then ligated into the *Kpn*I and *Xho*I sites of pSVF. All cDNAs were sequenced using an ABI 3100 capillary sequencer (Applied Biosystems).

Cell Culture and Transfection. C2C12 cells were grown in Dulbecco's modified Eagle medium containing 10% fetal bovine serum at 37 °C and 10% CO_2. Cells were transfected using Lipofectamine PLUS (Invitrogen, Carlsbad, CA), following the manufacturer's instructions. Cells were overlaid with the lipid−DNA complexes for approximately 23 h, the 5 first of which were in serum free OPTI-MEM media (Invitrogen). For immunofluorescence microscopy, transfections were performed directly in chamberslides (Nalge Nunc International, Naperville, IL). The cells were allowed to grow for approximately 48 h posttransfection before being prepared for immunofluorescence microscopy. For fluorescence recovery after photobleaching (FRAP) and fluorescence loss in photobleaching (FLIP), cells were transfected in dishes and split to chambered coverglasses (Nalge Nunc International) 29 to 48 h posttransfection. They were then grown for an additional 24 h before the photobleaching experiments.

Immunofluorescence Microscopy. Transfected cells were washed 3 times with phosphate-buffered saline (PBS) and then fixed with methanol for 6 min at −20 °C. The cells were permeabilized with 0.5% Triton X-100 in PBS for 2 min at room temperature, washed 3 times with 0.1% Tween-20 in PBS (solution A), and incubated with the primary antibodies diluted in PBS containing 0.1% Tween-20 and 2% bovine serum albumin (solution B) for 1 h at room temperature. The primary antibodies used were anti-FLAG M5 monoclonal antibody at a dilution of 1:200 (Sigma, St. Louis, MO) and anti-lamin B1 polyclonal antibody (*25*) at a dilution of 1:2000, or for GFP-tagged protein, anti-lamin B1 polyclonal antibody alone. After 4 washes with solution A, the cells were incubated with the secondary antibodies diluted 1:200 as described for the primary antibodies. Secondary antibodies used were lissamine rhodamine B conjugated goat anti-rabbit IgG and fluorescein isothiocyanate (FITC) conjugated goat anti-mouse IgG. The cells were then washed 4 times with solution A and 3 times with PBS. The slides were dipped in methanol and air-dried, and coverslips were mounted using SlowFade Light Anti-fade Kit (Molecular Probes, Eugene, OR). Immunofluorescence microscopy was performed on a Zeiss Axiovert 200 M microscope attached to a Zeiss LSM 510 confocal laser scanning system (Carl Zeiss, Inc., Thornwood, NY).

Fluorescence Photobleaching Experiments. FLIP and FRAP were performed on a Zeiss Axiovert 200 M microscope attached to a Zeiss LSM 510 confocal laser scanning system using the 488 nm line of a 30 mW argon laser in conjunction with a 40 × 0.9 N.A. objective. For FRAP, the bleached area was photobleached at full laser power (100% transmission) for 25 iterations, and recovery of photobleaching monitored by scanning at low power (5% transmission) in 2 s intervals. The average intensity of the fluorescence signal was measured in the region of interest using NIH Image J software (http://rsb.info.nih.gov/ij/). It was then normalized to the change in total fluorescence as $I_{rel} = T_0 I_t / T_t I_0$ where T_0 is total cellular intensity during prebleach, T_t total cellular intensity at time point t, I_0 the average intensity in the bleach region during prebleach, and I_t the average intensity in the bleach region at time point t (*26*). The normalized fluorescence was then plotted against time after bleach. To determine $t_{1/2}$, the time after bleach required for the fluorescence levels to reach the median between levels immediately after bleach and levels at steady state, we used the method described by Harrington et al. (*27*). We plotted $\ln(i_\infty - i_t)$ versus time after bleach, where i_t is the average normalized fluorescence intensity in the bleach region at time t and i_∞ the average normalized fluorescence intensity in the bleach region at infinity. The curves were fitted using MacCurveFit 1.5 (http://www.krs.com.au/mcf.html) and $t_{1/2}$ calculated as $t_{1/2} = \ln 2 \times (-1/\text{slope})$. Data from the first 10 s after bleach was used for all proteins except the slowly recovering emerin, where data from the first 60 s was used to give an accurate slope. The immobile fraction was calculated as $i_0 - i_\infty$, where i_0 is the average normalized fluorescence in the bleach region before bleach and i_∞ is the average normalized fluorescence in the bleach region at infinity.

For FLIP, the shape of the cell was determined by turning up the gain on the microscope enough to see the auto fluorescence of the cell. A small region outside the cell was then photobleached at full laser power (100% transmission) for 50 iterations, and photobleaching monitored by scanning

at low power (5% transmission). The area was bleached for 100 rounds of bleaching in 5.7 s intervals. The bleaching procedure was then repeated, bleaching first an area of the same size in the cytoplasm and finally an area of the same size in the nucleus. Average fluorescence in an area inside the nucleus, but outside the nuclear bleach region, was measured throughout all three bleach steps using NIH Image J software. The values were normalized as $I_{rel} = (I_t - b)/(I_0 - b)$ where I_t is the average fluorescence in the measured area at time t, I_0 the average fluorescence in the measured area at prebleach, and b the background fluorescence at the end of the experiment. The normalized fluorescence was then plotted against rounds of bleaching.

RESULTS

DUX1 and DUX4 Are Nuclear Proteins, Actively Transported into the Nucleus. To determine the intracellular localization of DUX1 and DUX4, we transiently transfected C2C12 mouse myoblasts with plasmids expressing these proteins. To enable detection of expressed proteins, FLAG-epitopes were fused to the amino termini of the constructs. Both DUX1 and DUX4 localized exclusively to the nucleus (Figure 1A). To detect DUX1 and DUX4 in live cells, we expressed the proteins fused to an enhanced form of GFP. Both DUX1-GFP and DUX4-GFP were exclusively nuclear, showing a similar localization to the FLAG-tagged proteins (Figure 1B).

While proteins smaller than 60 kDa can diffuse freely through the nuclear pore complex (NPC) into the nucleus (*28*), larger proteins must be actively transported through the nuclear pores. GFP is 27 kDa (*29*), giving fusion proteins of 46 kDa for DUX1-GFP and 72 kDa for DUX4-GFP. While DUX4-GFP clearly is above the size limit for passive diffusion into the nucleus, DUX1-GFP may be able to enter through the NPCs by diffusion. We therefore fused DUX1 to 2 consecutive GFP molecules (DUX1-2GFP), yielding a protein of 73 kDa. As DUX1-2GFP also was localized to the nucleus (Figure 1B), we conclude that both DUX1 and DUX4 are actively transported through the NPC.

The Nuclear Localization Signals of the DUX Proteins Are Situated within Their Homeodomains. The NLSs of most homeodomain proteins are situated within their homeodomains. To investigate if this is the case for the DUX proteins, and if both homeodomains are necessary and/or sufficient for this localization, we expressed chimeric proteins containing the different homeodomains with short flanking regions fused to GFP at their carboxyl termini. With the exception of the first homeodomain from DUX1 (DUX1 HD1), all constructs containing homeodomains localized to the nucleus (Figure 2A). The carboxyl-terminal tail of DUX4, distal to the second homeodomain, did not accumulate in the nucleus, but was not excluded from it. This protein, which when fused to GFP is approximately 53 kDa, may enter the nucleus by passive diffusion.

To determine if each of the nuclear homeodomains were localized through an active mechanism, we fused them to 2 consecutive GFP proteins, yielding proteins larger than 60 kDa. This did not affect their nuclear localization (Figure 2B), showing that the proteins are actively transported to the nucleus. The first homeodomain of DUX1 did not accumulate in the nucleus (Figure 2A). This domain differs

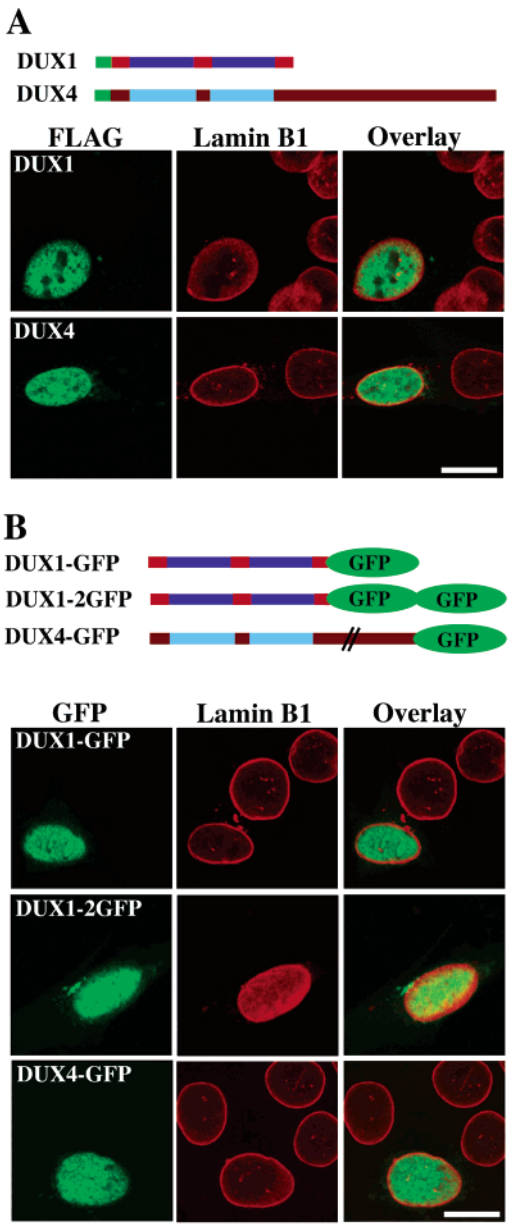

FIGURE 1: DUX1 and DUX4 are both localized to the nucleus, and their localizations are not affected by the addition of GFP to their carboxyl-termini. (A) Schematic diagrams show DUX1 and DUX4 with homeodomains shown in blue and the FLAG-tag in green (top). Panels show laser scanning confocal immunofluorescence microscopy images of C2C12 cells transiently transfected with plasmids that encode full-length DUX1 or DUX4 tagged with FLAG-tag and stained with monoclonal antibodies against FLAG, recognizing exogenous protein (left panels), and polyclonal anti-lamin B1 antibodies, recognizing endogenous lamin B1, a marker for the lamina/nuclear envelope (middle panels). The monoclonal antibodies were recognized by FITC-conjugated secondary antibodies, and the polyclonal antibodies were recognized by rhodamine-conjugated secondary antibodies. The panels to the right show an overlay of the FITC (green) and rhodamine (red) channels. (B) Schematic figures show DUX1 and DUX4 tagged with one or two molecules of GFP. Panels show confocal immunofluorescence microscopy images of C2C12 cells transiently transfected with full-length DUX1 or DUX4 tagged with GFP and stained with polyclonal anti-lamin B1 antibodies. The left panels show GFP fluorescence, the middle panels staining by rhodamine-conjugated secondary antibodies, recognizing anti-lamin B1 antibodies. The panels to the right show an overlay of the GFP (green) and rhodamine (red) channels. Bars: 10 μm.

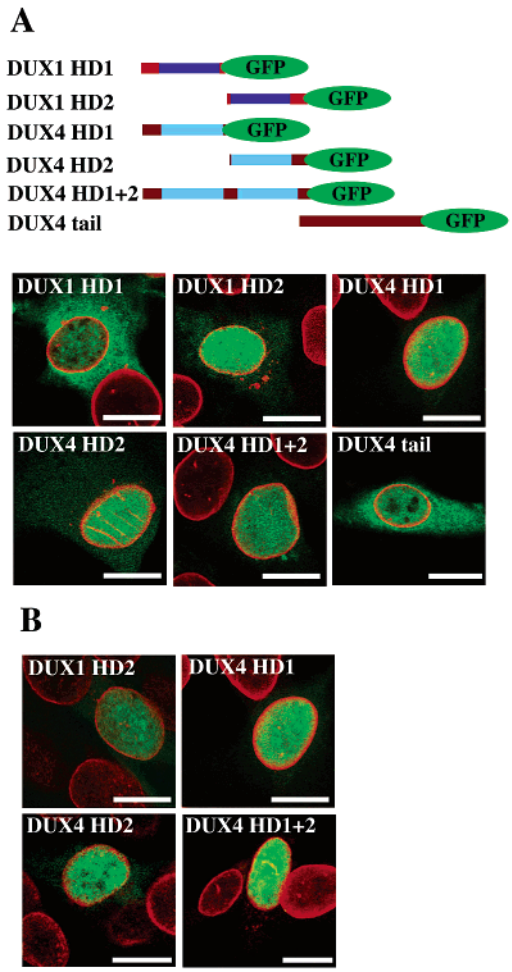

FIGURE 2: (A) The second homeodomain region of DUX1, as well as the first and second homeodomains of DUX4, accumulate in the nucleus, while the first homeodomain of DUX1 and the tail region of DUX4 do not. Schematic diagrams show truncated forms of DUX1 and DUX4 with homeodomains shown in blue and GFP in green (top). Panels show laser scanning confocal immunofluorescence microscopy images of C2C12 cells transiently transfected with cDNA encoding these proteins and stained with polyclonal anti-lamin B1 antibodies, recognizing endogenous lamin B1, a marker for the lamina/nuclear envelope. The panels show an overlay of GFP fluorescence and staining by rhodamine-conjugated secondary antibodies, recognizing anti-lamin B1 antibodies. (B) The domains that confer nuclear targeting of DUX proteins can be actively transported into the nucleus. Confocal immunofluorescence microscopy images of C2C12 cells expressing DUX1 or DUX4 protein domains fused to two consecutive GFP molecules, rendering the proteins to be large enough to require active transport into the nucleus, and stained as in panel A. Bars: 10 μm.

from the others by having fewer basic amino acids at its ends (see Discussion).

DUX1 Is More Mobile within the Nucleus than DUX4. To investigate the diffusional mobility of DUX1 and DUX4 in the nucleus, we performed FRAP. In these experiments, GFP-tagged proteins in an area in the nucleus of transiently transfected C2C12 myoblasts were irreversibly bleached using an argon laser at high power. The fluorescence recovery in the bleached area, corresponding to the influx of unbleached molecules from other areas, was then monitored. To exclude that the recovery of photobleaching monitored was due to reversible photobleaching of GFP, we performed control experiments on cells fixed with cold methanol for 6 min. No recovery was seen in these cells (Supplemental Figure 1A, Supporting Information). The recovery was also dependent on the photobleaching area (Supplemental Figure 1B), which would not be the case if the recovery were due to reversible photobleaching (*30*). As shown in Figure 3, both DUX1 and DUX4 recovered relatively rapidly. The recovery of DUX1 was, however, faster than that of DUX4 ($t_{1/2}$ for DUX1 was 4.8 s versus 13.4 s for DUX4). This difference was not only due to the larger size of DUX4, as DUX1 with 2 consecutive GFP molecules fused to its carboxyl-terminus, a protein of similar size as DUX4-GFP, was as mobile as DUX1-GFP (data not shown). It was not due to higher expression levels of DUX1 than DUX4, as the fluorescence recovery was significantly faster in cells expressing DUX1-GFP at a low level than in cells expressing DUX4-GFP at a high level (Supplemental Figure 2, Supporting Information). Both DUX1 and DUX4 had an immobile fraction of 10−15%. A truncated form of DUX4 lacking the carboxyl-terminal tail had a $t_{1/2}$ of recovery of 9 s. This protein encompasses the region homologous to DUX1, suggesting that the DUX4 homeodomains bind more strongly to a nuclear structure, for example DNA, than does DUX1. That truncated DUX4 diffused more rapidly than full-length DUX4 also suggests a role of the DUX4 carboxyl-terminal tail in the interaction between DUX4 and nuclear structures.

As shown in Figure 1, both DUX1 and DUX4 are concentrated in the cell nucleus. There is, however, a possibility that these proteins shuttle between the cytoplasm and the nucleus, albeit with much lower steady-state levels in the cytoplasm. To investigate this possibility, we performed FLIP. In this experiment, a region of the cell is repeatedly bleached, while the loss of fluorescence is monitored in another area of the cell. A loss of fluorescence in the unbleached area indicates that the fluorescent protein is free to move between the two areas. When an area of the cytoplasm was bleached, the loss of fluorescence from the nucleoplasm was no higher than when a region outside the cell but in close vicinity to the nucleus was bleached, indicating that there is no or very little flow of the DUX proteins out of the nucleus (Figure 4). When a region inside the nucleus was bleached, the rest of the nucleus lost its fluorescence, showing that the proteins are mobile within the nucleus, as indicated by the FRAP. The fluorescence in cells transfected with DUX1 was more rapidly lost than that in cells transfected with DUX4, confirming the FRAP data showing that DUX1 is more mobile within the nucleus than DUX4.

DISCUSSION

We have shown that the nuclear targeting signals of double homeodomain proteins are in the homeodomain region. This is consistent with reports for single homeodomain proteins. Several studies have shown that basic residues at the ends of the homeodomains are important for transport into the nucleus. The first homeodomain of DUX1 contains only 4 arginines/lysines in these regions, compared to 9 for the second homeodomains of DUX1 and 8 and 7 for the first and second homeodomain of DUX4, respectively (Figure 5). It is therefore not surprising that the first homeodomain of DUX1 was not actively imported into the nucleus.

Although the homeodomains from different proteins show a high degree of conservation, their NLSs are not identical.

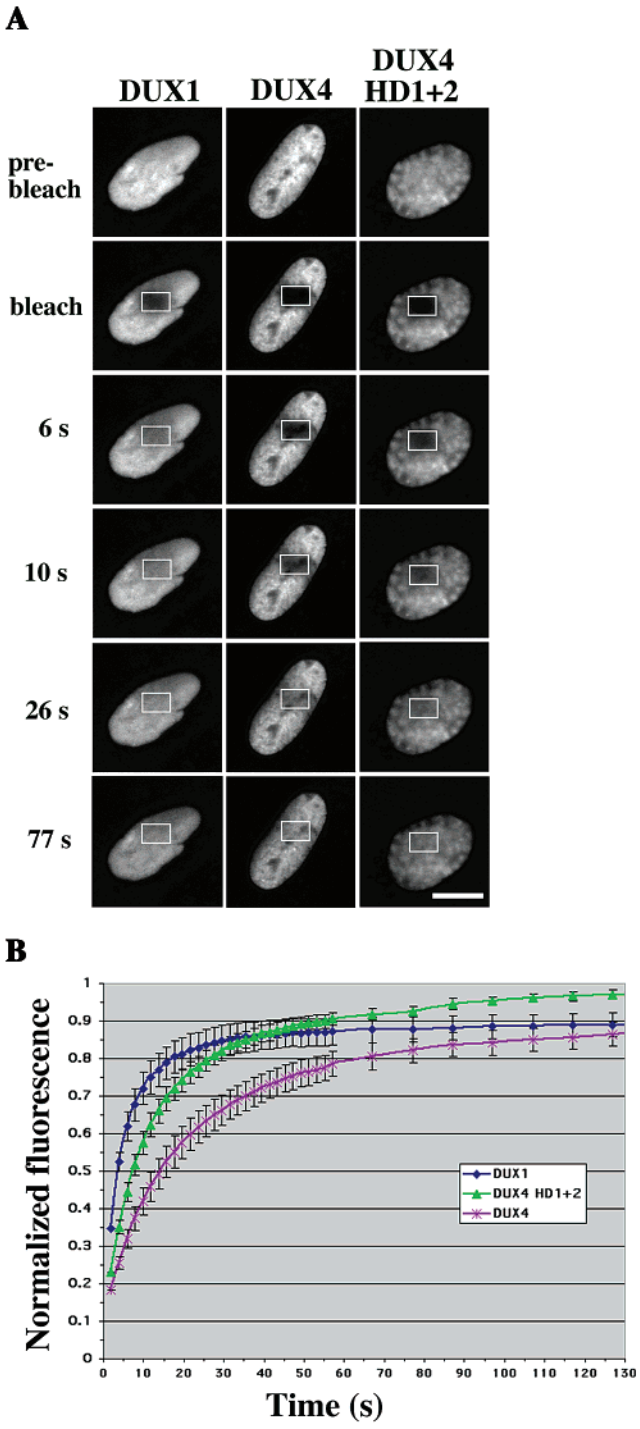

FIGURE 3: (A) The mobility of DUX1 is higher than that of DUX4, and full-length DUX4 is less mobile than DUX4 with the tail region deleted. Confocal fluorescence studies of mobilities of DUX1, DUX4, and DUX4 lacking the tail region (DUX4 HD1+2) by FRAP showing photobleach recovery in C2C12 cells transfected with proteins as labeled. The fluorescence in the boxed regions was bleached and recovery shown after 6, 10, 26, and 77 s after the bleaching. Bar: 5 μm. (B) Quantitative FRAP experiments showing normalized fluorescence recovery after photobleaching, where 1 is the fluorescence level before bleaching. The fluorescence intensity in the bleached region was measured and expressed as the relative recovery (see Experimental Procedures). The times for half-recovery were 4.8 s for DUX1, 13.4 s for DUX4, and 9 s for DUX4 lacking the tail region. Error bars indicate SEM, $n = 15$ for DUX1, 8 for DUX4, and 9 for DUX4 HD1+2.

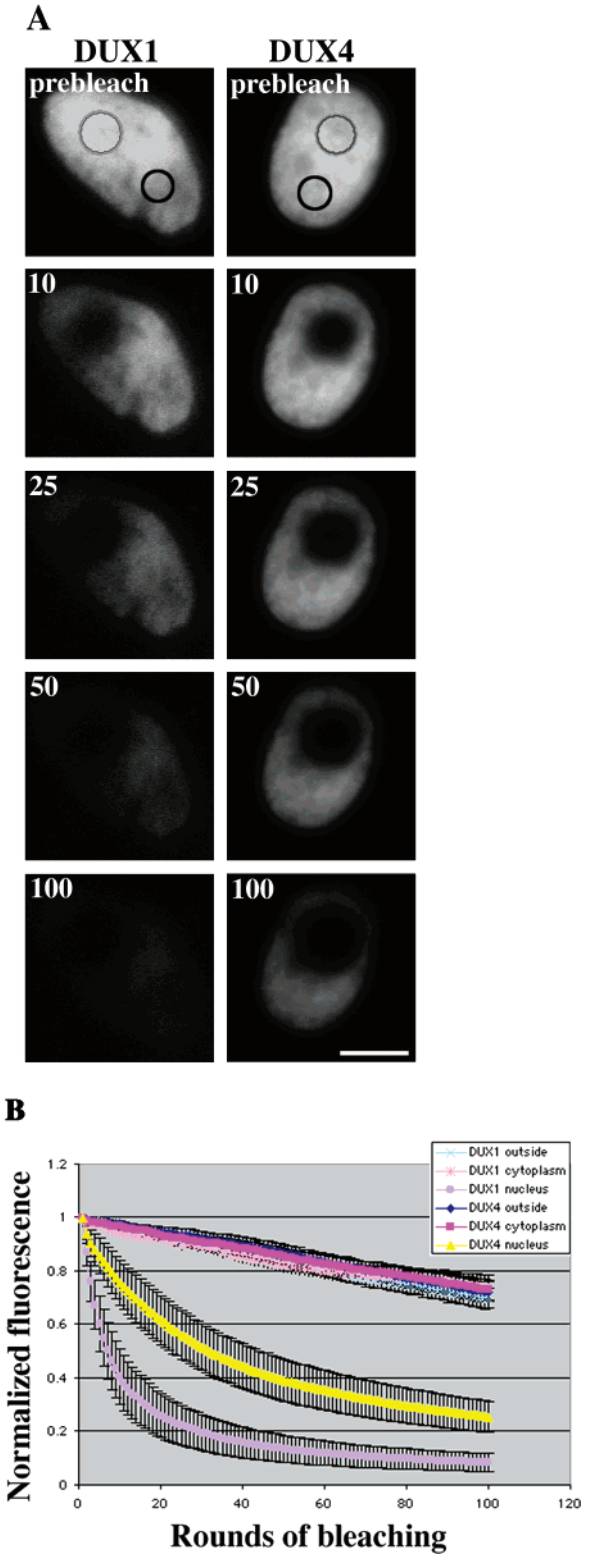

FIGURE 4: (A) FLIP experiment showing representative nuclei from cells expressing DUX1-GFP (left panels) or DUX4-GFP (right panels) bleached repeatedly in one area (gray circles) after 10, 25, 50, and 100 rounds of bleaching. The loss of fluorescence was measured in other areas of the cell nuclei (black circles). Bar: 5 μm. (B) Average fluorescence ($\pm$SEM, $n = 6$) in measured areas from cells bleached as shown in panel A (nucleus), or when an area of identical size from the cytoplasm of the cell (cytoplasm) or an area adjacent to the cell (outside) was bleached. While there was no difference between the loss of fluorescence in cells bleached in the cytoplasm or outside the cell, cells expressing DUX1 lost fluorescence significantly faster than cells expressing DUX4 when bleached in the nucleus.

FIGURE 5: Alignment using ClustalW (http://www.ebi.ac.uk/clustalw/) showing the homeodomains of DUX1 (two upper rows) and DUX4 (two lower rows), with basic residues shown in pink. "*" indicates identity between all sequences in the alignment, ":" indicates conserved substitutions, and "." indicates semiconserved substitutions. The terminal regions of the homeodomains, whose basic residues are important for nuclear localization (*22*), are shown in yellow. Notice that DUX1 HD1 has fewer such residues than the other homeodomains shown.

A common theme is, however, that basic residues at the ends of the homeodomain play important roles in nuclear targeting. PDX-1, a member of the *Antennapedia* class of homeodomain proteins, carries one NLS spanning 16 amino acids within the third alpha-helical segment, with 3 pairs of basic residues playing essential roles in the nuclear targeting (*17*). A similar NLS is found in the paired-bicoid protein PITX2, which also may contain another, weaker NLS in the amino-terminus of the homeodomain (*19*). Two sequences, in the beginning and the end of the homeodomain of Pax6, both contribute to the nuclear localization of this protein, which is imported into the nucleus by karyopherin 13 (*22*). Karyopherin 13 also imports Crx to the nucleus (*22*). Amino acids at the end of the homeodomain, which is highly homologous to Pax6, are important for this process (*18*, *22*). In the pairlike Vsx-1, the amino-terminus of the homeodomain contains an NLS (*31*).

To learn more about the dynamics of double homeodomain proteins within the cell nucleus, we performed fluorescence photobleaching experiments using GFP fusions. DUX1 and DUX4 were mobile within the nucleus, but did not shuttle between the nucleus and the cytoplasm to a significant extent. The times of half-recovery measured by FRAP (for DUX1 4.8 s and for DUX4 13.4 s) are on the same time-scale as those reported for other transcription factors, such as runt-related transcription factors 1 and 2 ($t_{1/2}$ = 10 s (*27*)) and HMG-17 ($t_{1/2}$ = 3 s (*26*)). The mobility of heterochromatin protein 1 (HP1) is different in euchromatin and heterochromatin, with $t_{1/2}$ being 4−5-fold lower in euchromatin (0.6 s (*32*); 10 s (*33*)) than in heterochromatin (2.5 s (*32*); 50 s (*33*)). The high mobility of HP1 suggests a transient binding and dynamic exchange of the protein despite the maintenance of stable, transcriptionally repressive heterochromatin structures (*32*, *33*). Integral nuclear membrane proteins of the inner nuclear envelope, such as emerin (*34*), MAN1 (*35*), and lamin B receptor (*36*), which interact with chromatin, exhibit a slower recovery rate than most nonmembrane chromatin-binding proteins. For emerin $t_{1/2}$ = 62 s has been reported (*37*). Under the same conditions used in the study of DUX proteins, we measured a $t_{1/2}$ of 49 s (data not shown). The lamin proteins, which constitute an intermediate filament network within nuclei, and also interact with chromatin (*38*), are extremely stable with $t_{1/2}$ for both lamin A and lamin B1 of >180 min (*39*), and no measurable recovery of lamin B1 45 h after bleaching in nondividing cells (*40*). Another very immobile protein is histone H2B, which showed little or no recovery under a 30 min period after bleaching, while the less tightly bound histone H1.1 has a $t_{1/2}$ of 18.7 s (*41*). These results suggest that proteins with a role in the structural organization of chromatin, such as histone H2B and lamins, have slow diffusion rates, while transcription factors such as homeodomain proteins have dynamic interactions and diffuse rapidly within the nucleus. Integral membrane proteins, such as emerin, which also may play a role in chromatin organization, show an intermediate level of mobility.

DUX1 was more mobile than DUX4 in the nucleus. This was not only due to the smaller size of DUX1, since the region of DUX4 homologous to DUX1 diffused less rapidly than DUX1. This suggests that the DUX4 homeodomains bind more strongly to some nuclear structure, such as DNA, than does DUX1. The carboxyl-terminal tail of DUX4 also seems to have transient interaction partners in the nucleus, since full-length DUX4 diffuses more slowly than the homeodomain region alone. Interestingly, the tail domain presented a very strong transcriptional activity upon fusion to the GAL4 DNA binding domain in the yeast simple hybrid system (*16*). In contrast, DUX1 did not show such activity (*16*) although it was previously shown to have transcriptional activity in a more sensitive cotransfection assay (*42*).

The gene encoding DUX4 is present in 3.3-kilobase repeats partially deleted in FSHD (*6*, *16*). These deletions have been reported to increase the expression of genes on chromosome 4q35 that are normally not expressed or expressed at low levels (*43*). The hypothesis has been put forward that DUX4 may not be expressed in normal muscle, but in muscle of individuals with FSHD, where it may be toxic to cells (*6*). DUX1, on the contrary, has been identified in several cell types (*5*, *7*, The Cancer Genome Anatomy Project http://cgap.nci.nih.gov). Differences between interaction partners or even slight differences in the strength of their interactions with DUX1 compared to DUX4 could help explain the putative toxicity of DUX4 to muscle cells, as the amounts of homeodomain proteins are strictly regulated and their overexpression perturbs cell functions (*4*).

ACKNOWLEDGMENT

We thank Sudhindra Swamy (Columbia University) for help with the photobleaching and confocal microscopy.

SUPPORTING INFORMATION AVAILABLE

Supplemental Figures 1 and 2. This material is available free of charge via the Internet at http://pubs.acs.org.

REFERENCES

1. Gehring, W. J., Affolter, M., and Bürglin, T. (1994) Homeodomain proteins, *Annu. Rev. Biochem. 63*, 487−526.
2. Lewis, E. B. (1978) A gene complex controlling segmentation in *Drosophila*, *Nature 276*, 565−570.
3. Cillo, C., Cantile, M., Faiella, A., and Boncinelli, E. (2001) Homeobox genes in normal and malignant cells, *J. Cell. Physiol. 188*, 161−169.
4. D'Elia, A. V., Tell, G., Paron, I., Pellizzari, L., Lonigro, R., and Damante, G. (2001) Missense mutations in human homeoboxes: a review, *Hum. Mutat. 18*, 361−374.
5. Ding, H., Beckers, M.-C., Plaisance, S., Marynen, P., Collen, D., and Belayew, A. (1998) Characterization of a double homeo-

domain protein (DUX1) encoded by a cDNA homologous to 3.3 kb dispersed repeated elements, *Hum. Mol. Genet. 7*, 1681−1694.
6. Gabriëls, J., Beckers, M.-C., Ding, H., De Vriese, A., Plaisance, S., van der Maarel, S. M., Padberg, G. W., Frants, R. R., Hewitt, J. E., Collen, D., and Belayew, A. (1999) Nucleotide sequence of the partially deleted D4Z4 locus in a patient with FSHD identifies a putative gene within each 3.3 kb element, *Gene 236*, 25−32.
7. Beckers, M.-C., Gabriëls, J., van der Maarel, S., De Vriese, A., Frants, R. R., Collen, D., and Belayew, A. (2001) Active genes in junk DNA? Characterization of *DUX* genes embedded within 3.3 kb repeated elements, *Gene 264*, 51−57.
8. Lee, J. H., Goto, K., Matsuda, C., and Arahata, K. (1995) Characterization of a tandemly repeated 3.3-kb *Kpn*I unit in the facioscapulohumeral muscular dystrophy (FSHD) gene region on chromosome 4q35, *Muscle Nerve 2*, S6−S13.
9. Galliot, B., de Vargas, C., and Miller, D. (1999) Evolution of homeobox genes: Q_{50} paired-like genes founded the paired class, *Dev. Genes Evol. 209*, 186−197.
10. Winokur, S. T., Bengtsson, U., Feddersen, J., Mathews, K. D., Weiffenbach, B., Bailey, H., Markovich, R. P., Murray, J. C., Wasmuth, J. J., Altherr, M. R., et al. (1994) The DNA rearrangement associated with facioscapulohumeral muscular dystrophy involves a heterochromatin-associated repetitive element: implications for a role of chromatin structure in the pathogenesis of the disease, *Chromosome Res. 2*, 225−234.
11. Lyle, R., Wright, T. J., Clark, L. N., and Hewitt, J. E. (1995) The FSHD-associated repeat, D4Z4, is a member of a dispersed family of homeobox-containing repeats, subsets of which are clustered on the short arms of the acrocentric chromosomes, *Genomics 28*, 389−397.
12. Wijmenga, C., Hewitt, J. E., Sandkuijl, L. A., Clark, L. N., Wright, T. J., Dauwerse, H. G., Gruter, A. M., Hofker, M. H., Moerer, P., Williamson, R., et al. (1992) Chromosome 4q DNA rearrangements associated with facioscapulohumeral muscular dystrophy, *Nat. Genet. 2*, 26−30.
13. van Deutekom, J. C., Wijmenga, C., van Tienhoven, E. A., Gruter, A. M., Hewitt, J. E., Padberg, G. W., van Ommen, G. J., Hofker, M. H., and Frants, R. R. (1993) FSHD associated DNA rearrangements are due to deletions of integral copies of a 3.2 kb tandemly repeated unit, *Hum. Mol. Genet. 2*, 2037−2042.
14. Hewitt, J. E., Lyle, R., Clark, L. N., Valleley, E. M., Wright, T. J., Wijmenga, C., van Deutekom, J. C., Francis, F., Sharpe, P. T., Hofker, M., et al. (1994) Analysis of the tandem repeat locus D4Z4 associated with facioscapulohumeral muscular dystrophy, *Hum. Mol. Genet. 3*, 1287−1295.
15. Paz, M. F., Wei, S., Cigudosa, J. C., Rodriguez-Perales, S., Peinado, M. A., Huang, T. H., and Esteller, M. (2003) Genetic unmasking of epigenetically silenced tumor suppressor genes in colon cancer cells deficient in DNA methyltransferases, *Hum. Mol. Genet. 12*, 2209−2219.
16. Coppée, F., Mattéotti, C., Anseau, E., Sauvage, S., Leclercq, I., Leroy, A., Marcowycz, A., Gerbaux, C., Figlewicz, D., Ding, H., and Belayew, A. (2004) The DUX gene family and FSHD, in *Facioscapulohumeral Muscular Dystrophy: Clinical Medicine and Molecular Biology* (Upadhyaya, M., and Cooper, D. N., Eds.) pp 117−134, Garland:BIOS Scientific Publishers, Abingdon, U.K.
17. Hessabi, B., Ziegler, P., Schmidt, I., Hessabi, C., and Walther, R. (1999) The nuclear localization signal (NLS) of PDX-1 is part of the homeodomain and represents a novel type of NLS, *Eur. J. Biochem. 263*, 170−177.
18. Fei, Y., and Hughes, T. E. (2000) Nuclear trafficking of photoreceptor protein Crx: the targeting sequence and pathologic implications, *Invest. Ophthalmol. Vis. Sci. 41*, 2849−2856.
19. Kozlowski, K., and Walter, M. A. (2000) Variation in residual PITX2 activity underlies the phenotypic spectrum of anterior segment developmental disorders, *Hum. Mol. Genet. 9*, 2131−2139.
20. Kaneko, H., Orii, K. O., Matsui, E., Shimozawa, N., Fukao, T., Matsumoto, T., Shimamoto, A., Furuichi, Y., Hayakawa, S., Kasahara, K., and Kondo, N. (1997) BLM (the causative gene of Bloom syndrome) protein translocation into the nucleus by a nuclear localization signal, *Biochem. Biophys. Res. Commun. 240*, 348−353.
21. Matsumoto, T., Shimamoto, A., Goto, M., and Furuichi, Y. (1997) Impaired nuclear localization of defective DNA helicases in Werner's syndrome, *Nat. Genet. 16*, 335−336.
22. Ploski, J. E., Shamsher, M. K., and Radu, A. (2004) Paired-type homeodomain transcription factors are imported into the nucleus by karyopherin 13, *Mol. Cell. Biol. 24*, 4824−4834.
23. Sambrook, J., Fritsch, E. F., and Maniatis, T. (1989) *Molecular Cloning: A Laboratory Manual*, 2nd ed., Cold Spring Harbor Laboratory Press, Cold Spring Harbor.
24. Saiki, R. K., Gelfand, D. H., Stoffel, S., Scharf, S. J., Higuchi, R., Horn, G. T., Mullis, K. B., and Erlich, H. (1987) Primer-directed enzymatic amplification of DNA with a thermostable DNA polymerase, *Science 239*, 487−491.
25. Cance, W. G., Chaudhary, N., Worman, H. J., Blobel, G., and Cordon-Cardo, C. (1992) Expression of the nuclear lamins in normal and neoplastic human tissue, *J. Exp. Clin. Cancer Res. 11*, 233−246.
26. Phair, R. D., and Misteli, T. (2000) High mobility of proteins in the mammalian cell nucleus, *Nature 404*, 604−609.
27. Harrington, K. S., Javed, A., Drissi, H., McNeil, S., Lian, J. B., Stein, J. L., Van Wijnen, A. J., Wang, Y. L., and Stein, G. S. (2002) Transcription factors RUNX1/AML1 and RUNX2/Cbfa1 dynamically associate with stationary subnuclear domains, *J. Cell Sci. 115*, 4167−4176.
28. Paine, P. L., Moore, L. C., and Horowitz, S. (1975) Nuclear envelope permeability, *Nature 254*, 109−114.
29. Prasher, D. C., Eckenrode, V. K., Ward, W. W., Prendergast, F. G., and Cormier, M. J. (1992) Primary structure of the *Aequorea victoria* green-fluorescent protein, *Gene 111*, 229−233.
30. Partikian, A., Ölveczky, B., Swaminathan, R., Li, Y., and Verkman, A. S. (1998) Rapid diffusion of green fluorescent protein in the mitochondrial matrix, *J. Cell Biol. 140*, 821−829.
31. Kurtzman, A. L., and Schechter, N. (2001) Ubc9 interacts with a nuclear localization signal and mediates nuclear localization of the paired-like homeobox protein Vsx-1 independent of SUMO-1 modification, *Proc. Natl. Acad. Sci. U.S.A. 98*, 5602−5607.
32. Cheutin, T., McNairn, A. J., Jenuwein, T., Gilbert, D. M., Singh, P. B., and Misteli, T. (2003) Maintenance of stable heterochromatin domains by dynamic HP1 binding, *Science 299*, 721−725.
33. Festenstein, R., Pagakis, S. N., Hiragami, K., Lyon, D., Verreault, A., Sekkali, B., and Kioussis, D. (2003) Modulation of heterochromatin protein 1 dynamics in primary mammalian cells, *Science 299*, 719−721.
34. Östlund, C., Ellenberg, J., Hallberg, E., Lippincott-Schwartz, J., and Worman, H. J. (1999) Intracellular trafficking of emerin, the Emery-Dreifuss muscular dystrophy protein, *J. Cell Sci. 112*, 1709−1719.
35. Wu, W., Lin, F., and Worman, H. J. (2002) Intracellular trafficking of MAN1, an integral protein of the nuclear envelope inner membrane, *J. Cell Sci. 115*, 1361−1372.
36. Ellenberg, J., Siggia, E. D., Moreira, J. E., Smith, C. L., Presley, J. F., Worman, H. J., and Lippincott-Schwartz, J. (1997) Nuclear membrane dynamics and reassembly in living cells: targeting of an inner nuclear membrane protein in interphase and mitosis, *J. Cell Biol. 138*, 1193−1206.
37. Shimi, T., Koujin, T., Segura-Totten, M., Wilson, K. L., Haraguchi, T., and Hiraoka, Y. (2004) Dynamic interaction between BAF and emerin revealed by FRAP, FLIP, and FRET analyses in living HeLa cells, *J. Struct. Biol. 147*, 31−41.
38. Stuurman, N., Heins, S., and Aebi, U. (1998) Nuclear lamins: their structure, assembly, and interactions, *J. Struct. Biol. 122*, 42−66.
39. Moir, R. D., Yoon, M., Khuon, S., and Goldman, R. D. (2000) Nuclear lamins A and B1: different pathways of assembly during nuclear envelope formation in living cells, *J. Cell Biol. 151*, 1155−1168.
40. Daigle, N., Beaudouin, J., Hartnell, L., Imreh, G., Hallberg, E., Lippincott-Schwartz, J., and Ellenberg, J. (2001) Nuclear pore complexes form immobile networks and have a very low turnover in live mammalian cells. *J. Cell Biol. 154*, 71−84.
41. Lever, M. A., Th'ng, J. P., Sun, X., and Hendzel, M. J. (2000) Rapid exchange of histone H1.1 on chromatin in living human cells, *Nature 408*, 873−876.
42. Ding, H., Descheemaeker, K., Marynen, P., Nelles, L., Carvalho, T., Carmo-Fonseca, M., Collen, D., and Belayew, A. (1996) Characterization of a helicase-like transcription factor involved in the expression of the human plasminogen activator inhibitor-1 gene, *DNA Cell Biol. 15*, 429−442.
43. Gabellini, D., Green, M. R., Tupler, R. (2002) Inappropriate gene activation in FSHD: a repressor complex binds a chromosomal repeat deleted in dystrophic muscle, *Cell 110*, 339−348.

BI047992W